Carbohydrate Polymers 81 (2010) 633–639

Contents lists available at ScienceDirect

Carbohydrate Polymers

journal homepage: www.elsevier.com/locate/carbpol

Effect of calcium ion (cross-linker) concentration on porosity, surface morphology and thermal behavior of calcium alginates prepared from algae (*Undaria pinnatifida*)

Tara Sankar Pathak, Jung-Ho Yun, Joonbae Lee, Ki-Jung Paeng*

Department of Chemistry, Yonsei University, Wonju 220-710, South Korea

ARTICLE INFO

Article history:
Received 6 January 2010
Received in revised form 3 March 2010
Accepted 11 March 2010
Available online 21 March 2010

Keywords:
Algae
Calcium alginates
Porosity
Surface morphology
Thermal degradation and kinetics

ABSTRACT

Alginic acid and metal (sodium) alginates was prepared from fresh algae using hot extraction method. Calcium alginates are also prepared from sodium alginate by varying calcium ion (calcium chloride) concentrations. FTIR spectra indicate that alginic acid is converted into metal alginate. Surface morphology as well as total intrusion volume, porosity (%) and pore size distribution changes by changing calcium ion (cross-linker) concentrations. Thermal degradation of calcium alginates showed a stepwise weight loss during thermal sweep, indicating different types of reactions during degradation. Calcium alginate (Calg0.6) prepared at low calcium ion concentration is least stable whereas at highest calcium ion concentration, the alginate sample (Calg20) is most stable at final degradation temperature (800 °C). Kinetic analysis was performed to fit with TGA data, where the entire degradation process has been considered as four consecutive 1st order reactions.

1. Introduction

Naturally occurring biopolymers like alginate, extracted from algae, have been known to exhibit excellent adsorption ability for metal ions (Abu Al-Rub, El Naas, Benyahia, & Ashour, 2004; Aksu, Eretli, & Kutsal, 1998; Angyal, 1989; Chanda, Hirst, Percival, & Ross, 1952; Chen, Tendeyong, & Yiacoumi, 1997; Muzzarelli, 1973).

Sodium alginate is the sodium salt of alginic acid which is a linear copolymer of (1-4)-linked β-d-mannuronic acid (M) and α-l-guluronic acid (G) residues as monomers, constituting M-, G-, and MG-sequential block structures (Chan, Jin, & Heng, 2002a; Haug, 1959; Moe, Draget, Skjak-Braek, & Smidrod, 1995). Since the M and G residues are in the $^4C_1$ and $^1C_4$ conformation, respectively, three types of glycosidic linkages are found generally in the block structures, including diequatorial (MM), diaxial (GG), and equatorial-axial (MG) (Funami et al., 2009). The G-block is stiffer and more extended in chain configuration than the M-block due to a higher degree of hindered rotation around the glycosidic linkages (Braccini, Grasso, & Perez, 1999).

Gelation of alginate is possible by interaction of carboxylate groups with divalent ions (Gombotz & Wee, 1998). Russso et al. reported that sodium alginates having different amount of guluronic fraction were ionically cross-linked with calcium ions in a fixed cross-linker (calcium chloride) concentration to form calcium alginate (Russo, Malinconico, & Santagata, 2007). Calcium cations are commonly used to cross-link sodium alginate. They have been reported to bind preferentially to the poly-guluronic acid units (GG) of alginate in a planar two-dimensional manner, producing the so-called "egg-box" structure (Chan, Lee, & Heng, 2002b; Grant, Morris, Rees, Smith, & Thom, 1973; Kohn & Furda, 1968; Morris, Rees, Thom, & Boyd, 1978; Rees & Welsh, 1977; Zheng, 1997). Alginates are very much important, due to their biodegradability, immunogenicity and ability to form gel with a variety of cross-linking agent (Roy, Bajpai, & Bajpai, 2009). These gels are used in various fields like food industry, medicine, and biotechnological applications including cell encapsulation and drug delivery (Kierstan & Bucke, 1977; Kneafsey, Shaughnessy, & Condon, 1996).

Now-a-days, the demand of natural polymer like alginate from renewable source has greatly increased, due to huge amount of plastic waste produced from synthetic polymer every year and the reduced availability of landfills. To reducing the problems of disposability of traditional plastics in landfills, biodegradable polymer (alginate) could be used in many applications instead of synthetic polymer.

Due to biodegradable nature and renewable resource of alginate, it could replace synthetic polymer in many applications. Therefore, their thermal degradation and kinetics is very much important.

Metal (calcium) ions with varying ion concentration usually affect the porosity, morphology, stability, etc.; which are also responsible for the degradation trend of calcium alginates. Thus, we

* Corresponding author. Tel.: +82 33 760 2239; fax: +82 33 760 2182.
E-mail address: paengk@yonsei.ac.kr (K.-J. Paeng).

0144-8617/$ – see front matter © 2010 Elsevier Ltd. All rights reserved.
doi:10.1016/j.carbpol.2010.03.025

Table 1
Preparation of Calcium alginate by varying calcium chloride concentration.

Sample name	Nalg (wt%)	$CaCl_2$ (wt%)
Calg0.6	1	0.6
Calg0.8	1	0.8
Calg2.5	1	2.5
Calg5	1	5
Calg7.5	1	7.5
Calg20	1	20

Nalg, sodium alginate; cross-linker, calcium chloride; cross-linker concentration, 0.6, 0.8, 2.5, 5, 7.5 and 20 wt%; Calg, calcium alginate.

have observed the effect of calcium ion (cross-linker) concentration on porosity, surface morphology and thermal behavior of calcium alginates prepared from algae (*Undaria pinnatifida*) in the present work. The kinetic analysis was also studied to fit thermogravimetric data by considering the whole process as four consecutive 1st order reactions.

2. Experimental

2.1. Materials used

Dried algae (*U. pinnatifida*, Sea mustard), a kind of brown seaweeds, Average molecular weight; 320 kDa, determined by viscometric methods, M/G ratio: 2.1 were supplied from Kyungsung University, Busan (South Korea). Sodium carbonate and cross-linker (calcium chloride) were obtained from Aldrich chemicals.

2.2. Preparation procedure of calcium alginates

Alginates were isolated from the algae in sodium form. Algae were processed at three principal regimes: (a) "cold" method, (b) "hot' method and (c) modified method including extraction in boiling state. Here, we used hot method for the extraction of alginate from algae (Pathak, Yun, Lee, Baek, & Paeng, 2009a). The extraction methods of alginate as well as preparation procedure of divalent metal (calcium) alginates are given below.

The dried algae 2 g was stirred with an alkali solution 1.5 wt% (sodium carbonate) for about 2 h at 50–60 °C. Alginate dissolves as sodium alginate to give very thick slurry (Pathak, Kim, Lee, Baek, & Paeng, 2008). This slurry also contains the part of the seaweed that does not dissolve, mainly cellulose. This insoluble residue removed from the solution by filtration. Sodium alginate is purified using solvent (water) and non-solvent (ethanol) method. The ratio of water and ethanol has been taken as 1:4 (v/v) in our experiment. Sodium alginate solution at a concentration of 1 wt% was prepared by dissolving the appropriate amount of sodium alginate in ultrapure water under magnetic stirring.

Sodium alginate solution is added drop wise to cross-linker ($CaCl_2$) solutions taken in a wide mouth glass jar to form calcium alginates. Calcium alginates were taken out of solution and washed with distilled water thoroughly to remove excess calcium chloride. After washing, calcium alginates were air-dried. The stoichiometric reaction between sodium alginate and calcium chloride is written as

$$2AlgCOONa + CaCl_2 \rightarrow (AlgCOO)_2Ca + 2NaCl$$

The composition of calcium alginates prepared by varying cross-linker concentration is presented in Table 1.

2.3. Preparation of alginic acid

The sodium alginate extract is treated with dilute mineral acid, HCl at room temperature and a gelatinous precipitate of alginic acid forms which cannot be filtered; it simply blocks any filter medium. It can be removed from the liquid by flotation. The detailed preparation procedure of alginic acid is also reported in our previous study (Pathak et al., 2008).

2.4. FTIR spectra of alginic acid and calcium alginates

Samples of alginic acid and calcium alginates were dried first and then ground before performing FTIR analysis. FTIR spectra were recorded on a Perkin-Elmer Spectrometer. The spectra were collected from 2000 to 800 cm^{-1} range in the transmission mode with 4 cm^{-1} resolution over 40 scans.

2.5. Scanning electron microscopy (SEM)

The surface properties of calcium alginates were studied using SEM. Specimen preparation was performed as follows: the dried sample was mounted on stubs and sputter-coated with gold. Micrographs were taken on a SEM instrument (Hitachi, S-4100).

2.6. Porosity

Calcium alginates samples were air-dried before porosity measurement. Pore diameter distribution, total intrusion volume and porosity were measured using auto pore IV 9500 V1.05 (Micromeritics Instrument Corporation, Norcross, GA, USA). Mercury filling pressure (1.33 psia) and equilibration time (10 s) was used in this study.

2.7. Thermogravimetric analysis (TGA)

Samples of calcium alginates were air-dried before doing TG analysis. Thermal analyses of samples were performed in the Universal V4.1D apparatus by heating up them from 18 to 800 °C with a heating rate of 10 °C/min under nitrogen atmosphere.

3. Results and discussion

In our study, wet calcium alginate bead had smooth surface and spherical shape whereas dried bead had rough surface at high calcium ion concentration (visualization); same observation was also reported by Polona, Marija, Anamarija, Odon, and Ales (2007). Ionic bonding between carboxylate groups of the sodium alginate with Ca^{2+} ions results in the formation of mechanically stable networks (Lee et al., 2000).

3.1. Fourier transform infrared spectroscopy

The stretching of C=O of protonated carboxylic group of alginic acid occurs at 1730 and 1609 cm^{-1}, respectively as it is seen in Fig. 1 (Pathak et al., 2009a,b). When the proton is displaced by a monovalent ion (sodium), the peaks appear at 1601 and 1432 cm^{-1}, respectively. These peaks are assigned for asymmetric and symmetric stretching vibration of free carboxyl group of sodium alginate. In the FTIR spectrum of alginic acid (Jeon, Nah, & Hwang, 2007), the peaks around 1030 cm^{-1} are attributed to the stretching of C–O–C.

Fig. 1 indicates that the peak at 1609 cm^{-1} for protonated carboxylic acid of alginic acid is shifted when proton is displaced by divalent metal (calcium) ion. As divalent metal ions replace sodium ions in the sodium alginate, the charge density, the radius and the atomic weight of the cation are changed, creating a new environment around the carbonyl group. Hence, a peak shift should be expected.

The alginate have carboxylate group which played an important role in binding metal ions. The percentage of ionic binding (PIB) can

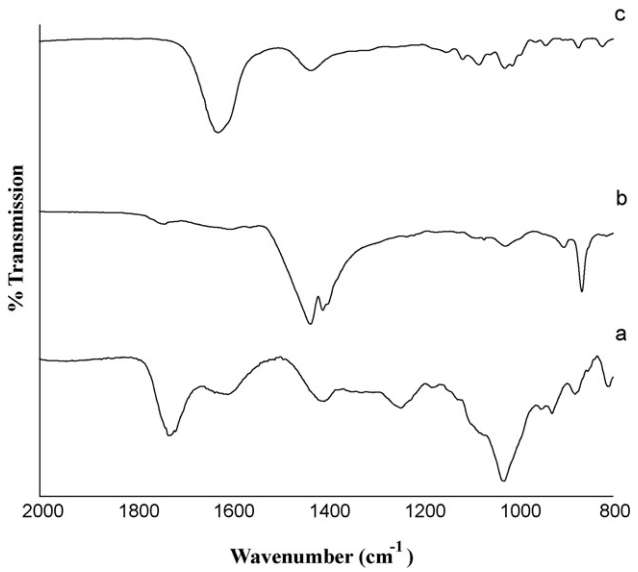

Fig. 1. FTIR spectra of (a) alginic acid, (b) sodium alginate and (c) calcium alginate (Calg20).

be calculated from the following formula (Chen, Hong, Wu, & Wang, 2002):

$$\text{PIB} = \frac{\nu_{(\text{COOH})} - \nu_{(\text{COOM})}}{\nu_{(\text{COOH})} - \nu_{(\text{COONa})}}$$

where ν is the frequency of asymmetric vibration of carboxylate group.

The denominator in the formula of PIB is the IR frequency shift of the asymmetric C=O vibration from the typical covalent bonding (carboxylic acid) to the typical ionic binding (sodium carboxylate), whereas its numerator term is the frequency shift of same vibration when a particular metal (M) ion is bound.

PIB was calculated on the basis of the frequencies obtained from FTIR analysis (Fig. 1). The values of frequencies of $\nu_{(\text{COOH})}$, $\nu_{(\text{COONa})}$ and $\nu_{(\text{COOCa})}$ are 1730, 1601 and 1627 cm^{-1}, respectively.

The PIB value of calcium alginate (Calg20) calculated using above formula is 0.798. The PIB value of calcium alginate is less than unity, due to higher metal carboxylate vibration frequencies compared to Na carboxylate.

3.2. Scanning electron microscopy

SEM was employed to determine the surface properties of calcium alginates by varying cross-linker concentration. The surface morphology of calcium alginates at 0.6, 0.8, 2.5, 5, 7.5 and 20 wt% of cross-linker concentration at fixed magnification are given in Fig. 2. SEM analysis revealed that surface morphology of calcium alginates changes by changing cross-linker concentration at same magnification. It is seen from SEM (Fig. 2) that at lowest concentration of cross-linker (Calg0.6), the pores were clearly shown whereas at highest concentration of cross-linker (Calg20), the pores were covered with dense layer of cross-linker. This can be explained on the basis of diffusion of Ca^{2+} ions from the core. As calcium chloride (cross-linker) concentration increases, the mass of calcium ions increases, resulted in a larger concentration gradient between the core and outside solution. This situation will favor the diffusion of Ca^{2+} ions from the core (Blandino, Macias, & Cantero, 1999). The crack was also observed in the dense layer of cross-linker in Calg20.

3.3. Porosity

Calcium alginates can be used in various fields, due to their wide variety of pore diameters varying from a few nanometers to several hundred nanometers. The total intrusion volume and porosity

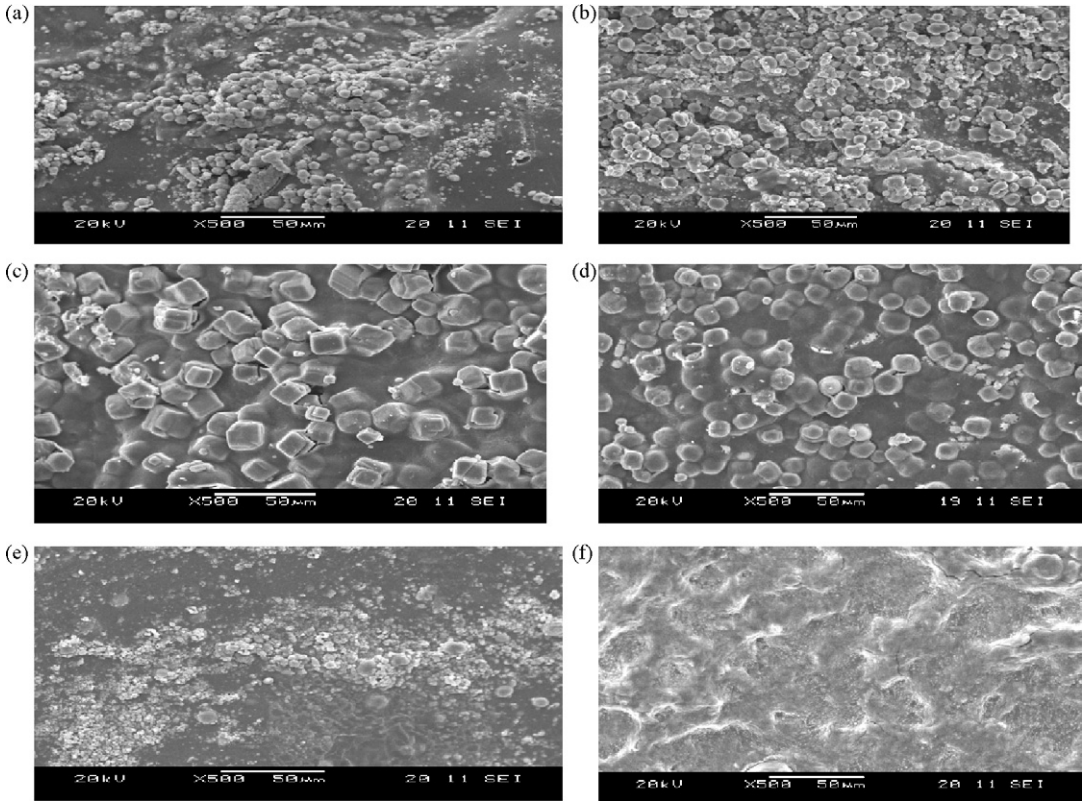

Fig. 2. Surface morphology of calcium alginate (a) Calg0.6, (b) Calg0.8, (c) Calg2.5, (d) Calg5, (e) Calg7.5 and (f) Calg20 by varying calcium chloride concentration.

Table 2
Pore characteristics of calcium alginates by varying calcium chloride concentration.

Sample name	Total intrusion volume (mL/g)	Bulk density (g/mL)	Apparent density (g/mL)	Porosity (%)
Calg2.5	0.0777 ± 0.0019	1.2706 ± 0.0317	1.4099 ± 0.0352	9.8782 ± 0.0034
Calg5	0.0530 ± 0.0011	1.7077 ± 0.0341	1.8775 ± 0.0375	9.0475 ± 0.0038
Calg7.5	0.0504 ± 0.0011	1.7384 ± 0.0382	1.9053 ± 0.0419	8.7595 ± 0.0014
Calg20	0.0394 ± 0.0008	1.9543 ± 0.0391	2.1173 ± 0.0423	7.7003 ± 0.0018

± Value refers to standard deviation.

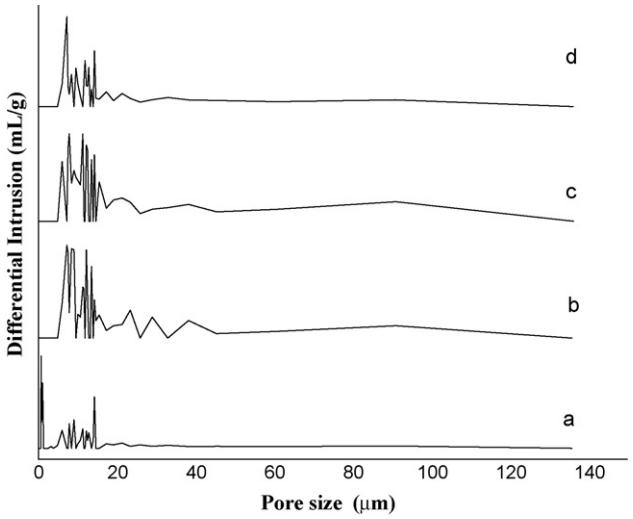

Fig. 3. Pore size distribution of calcium alginate by varying calcium chloride concentration (a) Calg2.5, (b) Calg5, (c) Calg7.5 and (d) Calg20.

(%) of calcium alginates by varying cross-linker concentration are given in Table 2. The total intrusion volume as well as porosity % of calcium alginates at higher concentration is lower compared to at lower concentration of cross-linker as it is seen in Table 2, due to more packed arrangement of alginate molecule at higher concentration of cross-linker. We observed in our previous study also (Pathak, Yun, Lee, Baek, & Paeng, 2009b) that with increase in cross-linker (zinc and cadmium) concentration, the total intrusion volume decreases. The same reason for decreasing total intrusion volume with increasing cross-linker concentration is applied in this study. A plot of pore size distribution (log differential intrusion against pore diameter) of calcium alginate is given in Fig. 3. The figure is showing that pore size distribution of calcium alginate changes by changing the cross-linker concentration.

3.4. Thermogravimetric analysis (TGA)

The thermogravimetric studies have been done with the various calcium alginate samples prepared using the calcium ion solutions of different concentrations to evaluate the exact variation in degradation trend of alginates with change in the metal ion concentrations. We further calculated the percentage weight loss values (P) from TGA graph (Fig. 4(A)), which are presented in Table 3. According to TG results, all the calcium alginate samples have followed the similar degradation trend with rise in the temperature, except the Calg20 sample. The rapid weight loss was taken place around 50–300 °C temperature in Calg20 sample and then the degradation rate became slower, and almost stopped after 600 °C. But, the percentage weight loss value at final temperature is much lower (52.8%) than those of other samples. On the other hand, all the other calcium alginates decomposed by different types of reactions during thermal sweeps, showing various steps in thermal degradation curves. It is seen that, the initial degradation took place around 50 °C, although rapid degradation process is situated around 200–700 °C, having three steps during these thermal sweeps. First step of rapid degradation was situated around 200–300 °C, followed by another step around 300–600 °C. It is known from literature that, there are three kinds of absorbed water in hydrophilic polymers (Hatakeyama, Hatakeyama, & Nakamura, 1995; Kim, Yoon, & Kim, 2004; Nakamura, Hatakeyama, & Hatakeyama, 1983), viz. free, freezing bound and non-freezing bound. Usually this free water does not react with the polymeric chain forming hydrogen bonding, behaves as pure water; whereas freezing bound water interacts weakly. But non-freezing bound water forms hydrogen bond to bind with polymeric chain. During the thermal sweep, these water molecules are first to leave the alginate samples. In our case, weight loss process took place with increasing temperature, when the decomposition processes were not yet involved (up to 200 °C). It means that, in addition to free water, the samples also contain the other two kinds of water, which were removed in a wide interval of temperature, before biopolymer degradation process took place. The first and second step of rapid degradation might be attributed to the biopolymer degradation process. The third step of rapid degradation was formed around 600–700 °C temperatures, which might have taken place due to the formation of metal carbonates. TG analysis had further performed up to 800 °C, where the decomposition rate becomes much slower.

It is worth noticing from the TG results that, Calg0.6 sample is thermally most unstable at final degradation temperature, whereas Calg20 is degraded least amount at 800 °C. It means that, the metal ion concentration during the preparation of alginate samples is responsible in variation of their thermal stability. Calcium alginate with much higher calcium concentration has shown considerable stability during thermal degradation; although, moderate change in the metal ion concentration did not always follow the same trend.

Table 3
Thermal analysis of calcium alginates (Calg0.6, Calg0.8, Calg2.5, Calg5, Calg7.5 and Calg20) by varying calcium chloride concentrations at heating rate of 10 °C/min in nitrogen atmosphere.

Temp. (°C)	Calg0.6%wt loss	Calg0.8%wt loss	Calg2.5%wt loss	Calg5% wt loss	Calg7.5%wt loss	Calg20%wt loss
100	7.97	6.95	6.19	5.20	7.67	22.19
200	14.46	12.82	10.78	12.13	13.15	37.05
300	37.81	35.98	28.81	30.25	36.22	43.09
400	43.14	41.35	33.78	35.78	42.19	45.21
500	48.00	46.24	37.49	39.53	46.97	46.17
600	51.79	47.59	38.78	41.09	48.16	50.03
700	64.15	57.71	54.99	56.36	57.37	51.39
800	77.67	67.59	62.64	62.02	65.84	52.86

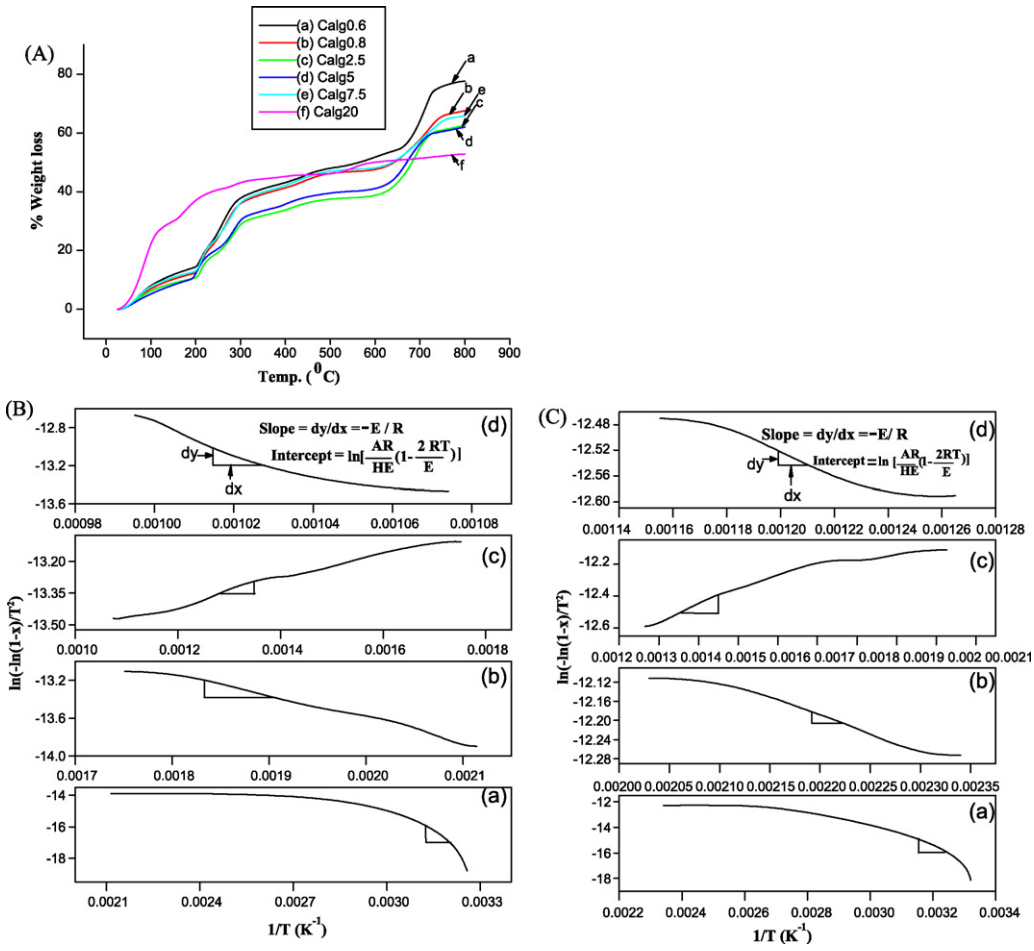

Fig. 4. (A) TGA graph of calcium alginate (a) Calg0.6, (b) Calg0.8, (c) Calg2.5, (d) Calg5, (e) Calg7.5 and (f) Calg20 by varying calcium chloride concentration. (B) Plot of $\ln[-\ln(1-X)/T^2]$ vs. $1/T$ at heating rate of 10 °C/min in the temperature range (a) 307–473 K, (b) 473–571 K, (c) 571–931 K and (d) 931–1005 K from TGA data for calcium alginate sample (Calg0.6). (C) Plot of $\ln[-\ln(1-X)/T^2]$ vs. $1/T$ at heating rate of 10 °C/min in the temperature range: (a) 301–427 K, (b) 427–492 K, (c) 492–787 K and (d) 787–862 K from TGA data for calcium alginate sample (Calg20).

Complex formation nature between metal ion and functional group on the alginate surface was complicated and difficult to understand; thus thermal degradation behavior of metal alginates is not still clear to us. We reported in our previous study that the percent weight loss at 100 °C is 1.43 for Calg10 sample whereas in this study the weight loss at 100 °C for Calg0.6, Calg0.8, Calg2.5, Calg5, Calg7.5 and Calg20 are 7.97, 6.95, 6.19, 5.20, 7.67 and 22.19% respectively. The weight loss at 100 °C mainly, due to the physical loss of moisture from the alginates sample. Moisture loss from alginate samples cannot control because of complicated complex formation nature of alginate samples as already stated above. The irregular weight loss of alginate samples by varying calcium chloride concentrations due to irregular moisture loss from the sample.

3.4.1. Kinetic analysis

Kinetic parameters (activation energy and pre-exponential factor) of thermal degradation processes of calcium alginate samples using different concentration of calcium ion were calculated using integral method (Coats & Redfern, 1964). The whole process of thermal degradation was divided into four subsequent steps, and each step was taken into account as 1st order reaction. Therefore, the kinetic equation for each step can be written using following expression:

$$\frac{dx}{dt} = A\exp\left(\frac{-E}{RT}\right)(1-x) \quad (1)$$

The integrated form of Eq. (1) at a constant heating rate $H(=dT/dt)$ can be written as

$$\ln\left[\frac{-\ln(1-X)}{T^2}\right] = \ln\left[\frac{AR}{HE}\left(1-\frac{2RT}{E}\right)\right] - \frac{E}{RT} \quad (2)$$

The meaning of term A, E, T, t and x as well as determination procedure of activation energy (E) and pre-exponential factor (A) are already reported in previous research (Chattopadhyay, Kim, Kim, & Pak, 2008; Pathak et al., 2009a,b; Zhou, Wang, Huang, & Cai, 2006).

In Fig. 4(B and C), $\ln[-\ln(1-x)/T^2]$ vs. $1/T$ was plotted for Calg0.6 and Calg20 samples using 10 °C/min heating rate in thermal degradation process. Here, the entire process was divided into four consecutive 1st order reactions. So, Eq. (1) is applied for every single step and the plots have come out essentially with straight line. The value of x was calculated separately for each step. The value of kinetic parameters in Table 4 for all the samples are written for $x = 0.02$–0.06% to 49.8–77.35%, which is the main conversion range for all the calcium alginate samples.

First and last step of degradation processes are containing higher activation energy values as it is seen in Table 4, whereas third step has shown negative E value for all the calcium alginates. Negative activation energy is the one in which, reaction rate decreases with increasing temperatures and these reactions are typically barrierless reactions whereas reaction with high activation energy requires a high temperature or a long residence time (Lazaro, Moliner, & Suelves, 1998). High activation energy means

Table 4
Kinetics parameters of Calg0.6, Calg0.8, Calg2.5, Calg5, Calg7.5 and Calg20 obtained from TGA analysis.

Sample name	Heating rate (°C/min)	Temp. (K)	Conversion range (%)	E (kJ/mol)	A (min^{-1})
Calg0.6	10	307–473	0.02–13.89	138.566	450
	10	473–571	13.89–38.65	18.4755	0.12
	10	571–931	38.65–53.64	−5.9385	514
	10	931–1005	53.64–77.35	103.925	0.40
Calg0.8	10	305–473	0.07–12.82	118.771	142.0
	10	473–576	12.82–36.28	18.475	0.1210
	10	576–903	36.28–48.99	−10.392	0.0092
	10	903–1051	48.99–66.87	103.925	0.7640
Calg2.5	10	304–476	0.03–11.07	81.310	3.83
	10	476–581	11.07–29.72	16.628	0.108
	10	581–900	29.72–40.29	−13.856	0.0011
	10	900–1061	40.29–62.24	92.377	1.14
Calg5	10	304–463	0.06–10.28	118.771	142.0
	10	463–583	10.28–31.43	16.628	0.1095
	10	583–909	31.43–43.52	−0.923	0.0001
	10	909–1058	43.52–61.55	87.515	0.7980
Calg7.5	10	303–470	0.05–12.86	118.771	52.4
	10	470–571	12.86–35.89	16.628	0.104
	10	571–903	35.89–49.43	−10.392	0.008
	10	903–1040	49.43–65.04	41.570	0.155
Calg20	10	301–427	0.05–30.33	83.14	733
	10	427–492	30.33–38.88	4.157	0.051
	10	492–787	38.88–46.46	−10.39	0.024
	10	787–862	46.46–49.80	16.628	0.134

that the reaction needs more energy from the surroundings during the reaction, for thermal degradation process. The Calg0.6 sample has shown the highest E value (138.56 kJ/mol) at the first step of thermal process considering each step as 1st order reaction. Although in this case, the E values did not show any dependence on the metal ion concentration in the alginate samples. The kinetic parameters were calculated up to 50% conversion range for Calg20 sample, because after that this alginate sample did not degrade much.

4. Conclusions

Alginic acid and metal alginate was prepared from algae using hot extraction method. The formation of alginic acid and metal alginates were confirmed by FTIR spectroscopy. The variation of calcium ion (cross-linker) concentrations had been affected the surface morphology at same magnification of calcium alginate samples (Calg0.6, Calg0.8, Calg2.5, Calg5, Calg7.5 and Calg20).

Similarly, total intrusion volume, porosity percentage and pore size distribution of alginate samples had been varied with changes in the cross-linker concentration. Calcium alginates had degraded in various steps and showed a stepwise weight loss during thermal sweep, indicating different types of reactions during thermal degradation. At final degradation temperature (800 °C), Calcium alginate (Calg20) is most thermally stable at high calcium ion concentration whereas Calg0.6 at low calcium ion concentration is least stable. Kinetic analysis reveals that thermal degradation of calcium alginates shows four consecutive 1st order reactions for the different subintervals of weight loss found quite satisfactorily with the Arrhenius law. Due to biodegradable nature and renewable resource of alginate, it can be used instead of synthetic polymer in many applications.

Acknowledgement

This study was supported by a Grant of Korea Institute of Marine Science & Technology Promotion (KIMST), South Korea.

References

Abu Al-Rub, F. A., El Naas, M. H., Benyahia, F., & Ashour, I. (2004). Biosorption of nickel on blank alginate beads, free and immobilized algal cells. *Process Biochemistry*, *39*(11), 1767–1773.

Aksu, Z., Eretli, G., & Kutsal, T. A. (1998). Comparative study of copper(II) biosorption on Ca-alginate, agarose and immobilized *C. vulgaris* in a packed-bed column. *Process Biochemistry*, *33*(4), 393–400.

Angyal, S. J. (1989). Complexes of metal cations with carbohydrates in solution. *Advances in Carbohydrate Chemistry and Biochemistry*, *47*, 1–43.

Blandino, A., Macias, M., & Cantero, D. (1999). Formation of calcium alginate gel capsules: Influence of sodium alginate and $CaCl_2$ concentration on gelation kinetics. *Journal of Bioscience and Bioengineering*, *88*(6), 686–689.

Braccini, I., Grasso, R. P., & Perez, S. (1999). Conformational and configurational features of acidic polysaccharides and their interactions with calcium ions: A molecular modeling investigation. *Carbohydrate Research*, *317*(1–4), 119–130.

Chan, L. W., Jin, Y., & Heng, P. W. S. (2002). Cross-linking mechanisms of calcium and zinc in production of alginate microspheres. *International Journal of Pharmaceutics*, *242*(1–2), 255–258.

Chan, L. W., Lee, H. Y., & Heng, P. W. S. (2002). Production of alginate microspheres by internal gelation using an emulsification method. *International Journal of Pharmaceutics*, *242*(1–2), 259–262.

Chanda, S. K., Hirst, E. L., Percival, B. G. V., & Ross, A. G. (1952). The structure of alginic acid. Part II. *Journal of Chemical Society*, 1833–1837.

Chen, J. P., Hong, L., Wu, S., & Wang, L. (2002). Elucidation of interactions between metal ions and Ca alginate-based ion-exchange resin by spectroscopic analysis and modeling simulation. *Langmuir*, *18*(24), 9413–9421.

Chen, J. P., Tendeyong, F., & Yiacoumi, S. (1997). Equilibrium and kinetic studies of copper ion uptake by calcium alginate. *Environmental Science and Technology*, *31*(5), 1433–1439.

Chattopadhyay, J., Kim, C., Kim, R., & Pak, D. (2008). Thermogravimetric characteristics and kinetic study of biomass co-pyrolysis with plastics. *Korean Journal of Chemical Engineering*, *25*(5), 1047–1053.

Coats, A. W., & Redfern, J. F. (1964). Kinetic parameters from thermogravimetric data. *Nature*, *201*(4914), 68–69.

Funami, T., Fang, Y., Noda, S., Ishihara, S., Nakauma, M., Draget, K. I., et al. (2009). Rheological properties of sodium alginate in an aqueous system during gelation in relation to supermolecular structures and Ca^{2+} binding. *Food Hydrocolloids*, *23*(7), 1746–1755.

Gombotz, W., & Wee, S. W. (1998). Protein release from alginate matrices. *Advanced Drug Delivery Reviews*, *31*(3), 267–285.

Grant, G. T., Morris, E. R., Rees, D. A., Smith, P. J., & Thom, C. D. (1973). Biological interactions between polysaccharides and divalent cations: The egg-box model. *FEBS Letters*, *32*(1), 195–198.

Hatakeyama, T., Hatakeyama, H., & Nakamura, K. (1995). Non-freezing water content of mono- and divalent cation salts of polyelectrolyte–water systems studied by DSC. *Thermochimica Acta*, *253*, 137–148.

Haug, A. (1959). Fractionation of alginic acid. *Acta Chemica Scandinavica*, *13*, 601–603.

Jeon, C., Nah, I. W., & Hwang, K. Y. (2007). Adsorption of heavy metals using magnetically modified alginic acid. *Hydrometallurgy*, *86*(3–4), 140–146.

Kierstan, M., & Bucke, C. (1977). The immobilization of microbial cells, subcellular organelles, and enzymes in calcium alginate gels. *Biotechnology and Bioengineering*, *19*(3), 387–397.

Kim, S. J., Yoon, S. G., & Kim, S. I. (2004). Synthesis and characteristics of interpenetrating polymer network hydrogels composed of alginate and poly(diallydimethylammonium chloride). *Journal of Applied Polymer Science*, *91*(6), 3705–3709.

Kneafsey, B., Shaughnessy, M. O., & Condon, K. C. (1996). The use of calcium alginate dressings in deep hand burns. *Burns*, *22*(1), 40–43.

Kohn, R., & Furda, I. (1968). Binding of calcium ions to acetyl derivatives of pectin. *Collection of Czechoslovak Chemical Communications*, *33*, 2217–2225.

Lazaro, M. J., Moliner, R., & Suelves, I. (1998). Non-isothermal versus isothermal technique to evaluate kinetic parameters of coal pyrolysis. *Journal of Analytical and Applied Pyrolysis*, *47*(2), 111–125.

Lee, K. Y., Rowley, J. A., Eiselt, P., Moy, E. M., Bouhadir, K. H., & Mooney, D. J. (2000). Controlling mechanical and swelling properties of alginate hydrogels independently by cross-linker type and cross-linking density. *Macromolecules*, *33*(11), 4291–4294.

Moe, S. T., Draget, K. I., Skjak-Braek, G., & Smidrod, O. (1995). Alginates. In A. M. Stephen (Ed.), *Food polysaccharides and their applications* (pp. 245–286). New York: Marcel-Dekker.

Morris, E. R., Rees, D. A., Thom, D., & Boyd, J. (1978). Chiroptical and stoichiometric evidence of a specific, primary dimerisation process in alginate gelation. *Carbohydrate Research*, *66*(1), 145–154.

Muzzarelli, R. A. A. (1973). *Natural chelating polymers international series of monographs in analytical chemistry*. Oxford, UK: Pergamon Press.

Nakamura, K., Hatakeyama, T., & Hatakeyama, H. (1983). Relationship between hydrogen bonding and bound water in polyhydroxystyrene derivatives. *Polymer*, *24*(7), 871–876.

Pathak, T. S., Kim, J. S., Lee, S. J., Baek, D. J., & Paeng, K. J. (2008). Preparation of alginic acid and metal alginate from algae and their comparative study. *Journal of Polymers and the Environment*, *16*(3), 198–204.

Pathak, T. S., Yun, J. H., Lee, S. J., Baek, D. J., & Paeng, K. J. (2009a). Effect of cross-linker and cross-linker concentration on porosity, surface morphology and thermal behavior of metal alginates prepared from algae (*Undaria pinnatifida*). *Carbohydrate Polymers*, *78*(3), 717–724.

Pathak, T. S., Yun, J. H., Lee, S. J., Baek, D. J., & Paeng, K. J. (2009b). Effect of solvent composition on porosity, surface morphology and thermal behavior of metal alginate prepared from algae (*Undaria pinnatifida*). *Journal of Polymers and the Environment*, doi:10.1007/s10924-009-0156-5

Polona, S., Marija, B., Anamarija, Z., Odon, P., & Ales, M. (2007). Shape optimization and characterization of polysaccharide beads prepared by ionotropic gelation. *Journal of Microencapsulation*, *25*(2), 90–105.

Rees, D. A., & Welsh, E. J. (1977). Secondary and tertiary structure of polysaccharides in solutions and gels. *Angewandte Chemie International Edition in English*, *16*(4), 214–224.

Roy, A., Bajpai, J., & Bajpai, A. K. (2009). Dynamics of controlled release of chlorpyrifos from swelling and eroding biopolymeric microspheres of calcium alginate and starch. *Carbohydrate Polymers*, *76*(2), 222–231.

Russo, R., Malinconico, M., & Santagata, G. (2007). Effect of cross-linking with calcium ions on the physical properties of alginate films. *Biomacromolecules*, *8*, 3193–3197.

Zheng, H. (1997). Interaction mechanism in sol–gel transition of alginate solutions by addition of divalent cations. *Carbohydrate Research*, *302*(1–2), 97–101.

Zhou, L., Wang, Y., Huang, Q., & Cai, J. (2006). Thermogravimetric characteristics and kinetic of plastic and biomass blends co-pyrolysis. *Fuel Processing Technology*, *87*(11), 963–969.